JOURNAL OF APPLIED ELECTROCHEMISTRY 12 (1982) 27–38

Studies concerning charged nickel hydroxide electrodes. VI. Voltammetric behaviour for pre-cycled electrodes

R. BARNARD, C. F. RANDELL

Berec Group Limited, Group Technical Centre, St. Ann's Road, London, UK

Received 14 April 1982

In this study cyclic voltammetry/coulometry has been combined with oxygen volume measurements to identify the species giving the multiple anodic and cathodic peaks for a pre-cycled β-$Ni(OH)_2$ starting material. A complex sequence of 1 and 2 electron transfer reactions involving several U_α/V_α and U_β/V_β coexisting phase pairs has been identified. This system is complicated by overlap of the various processes in some cases and also the chemical transformation of unstable α-phases. As many as six anodic and four cathodic processes can be encountered depending on the charging history.

1. Introduction

In a previous paper [1] it was shown that by restricting the anodic limit and the charge applied to β-$Ni(OH)_2$ that the oxidized phases also remained within the β-phase system. At low average oxidation states (2.1–2.2) a single broad cathodic peak appeared at $\approx$ 400 mV ascribed to the reduction of coexisting phase V_β, i.e., $[0.9NiOOH \cdot 0.1Ni(OH)_2]0.21H_2O \cdot 0.03KOH$, to phase U_β, i.e., $[0.25NiOOH \cdot 0.75Ni(OH)_2]$ $0.25H_2O$. When the average oxidation state was increased progressively to 2.7 then the reduction process was found to shift to more cathodic potentials in the range 350–300 mV.

Shifts in the cathodic peak potential were found to be related to changes in quasi-reversible potential for the species present. The range of reduction potentials for oxidized β-phases was considered to be due to differences in free energy between various pairs of coexisting phases U_β and V_β which are present within the β-phase layer lattice system [2–6].

The purpose of this investigation was to examine in more detail the voltammetric behaviour of electrodes which have been previously charged to give the γ-phase, V_α, i.e. $[0.833NiO_2 \cdot 0.166Ni(OH)_2]0.35H_2O \cdot 0.33KOH$ or $K_{0.33}NiO_2 \cdot 0.67H_2O$ and then discharged. As will be shown in this communication subsequent oxidation/reduction cycles may involve a complex mixture of coexisting phases of the general types U_α, U_β, V_γ and V_β having different free energies of formation.

2. Experimental procedure

2.1. *Techniques*

The linear sweep voltammetry/coulometry technique coupled with simultaneous measurement of oxygen volumes has been described in detail in the previous study [1].

2.2. *Electrode materials and pre-treatment*

The sintered plate electrodes were of the types A and B designated previously [1] containing well crystallized β-$Ni(OH)_2 \cdot 0.25H_2O$. These electrodes contained $\approx$ 0.09 g of active material in a sample size 1 cm x 1 cm.

Some electrodes were pre-cycled voltammetrically (4 cycles between 550 and 50 mV with respect to Hg/HgO/7 mol dm^{-3} KOH at 10 mV min^{-1}) such that the maximum oxidation state reached was 2.65. After reduction, the electrodes had a residual oxidation state of 2.32 and were used in this state as the starting material for part of this study. X-ray diffraction confirmed that only β-phase materials were present in the treated samples.

Other electrodes were charged galvanostatically at the C/2 rate for 12 h until an oxidation state of $\approx$ 3.5 had been reached [7]. Electrodes of this type

0021–891X/83/010027–12$03.94/0

have been shown by X-ray diffraction to contain only the phase V_γ, ($K_{0.33}NiO_2 0.67H_2O$). These electrodes were then discharged by a cathodic linear potential scan at 20 or 10 mV min^{-1}. The electrodes containing residual γ-phase had an oxidation state of ≈ 2.65. Throughout this study potentials are referred to Hg/HgO/7 mol dm^{-3} KOH at 22° C and 7 mol dm^{-3} KOH was used as electrolyte.

3. Results and discussion

3.1. *Cyclic voltammetry*

Figure 1 shows a sequence of cyclic voltammograms obtained between limits of 650 and 150 mV at a sweep rate of 10 mV min^{-1} for a sintered plate electrode containing chemically precipitated β-$Ni(OH)_2$ designated type A in the previous study [1]. The first point to note is that the shape of the first anodic scan is entirely different from those on the later cycles 2–4, but the corresponding cathodic curves are very similar on all cycles. In the previous study [1] the first cycle behaviour was studied in detail. Coulometric and X-ray diffraction methods revealed that the first peak at 540 mV as in Fig. 1 was due to oxidation of β-$Ni(OH)_2$ to β-NiOOH or using co-existing phase notation [2–6] β-$Ni(OH)_2 \cdot 0.25H_2O \rightarrow$ phase $U_\beta \rightarrow$ phase V_β where U_β denotes the least oxidized coexisting phase and V_β the more oxidized. Removal of the oxygen evolution current component at high anodic potentials allowed a further peak at ≈ 610 mV (not observable directly in Fig. 1) to be seen arising from further oxidation of β-NiOOH to the γ-phase V_γ, $K_{0.33}NiO_2 0.67H_2O$. The single reduction peak at ≈ 250 mV is ascribed entirely to reduction of the γ-phase (V_γ) to an α-phase (U_α). The phase U_α, i.e., $[0.125NiO_2 \cdot 0.875Ni(OH)_2]0.67H_2O$ related to the α-$Ni(OH)_2$ crystal structure is unstable and reverts chemically to the more stable β-phase, U_β on standing in alkaline solution.

The purpose of this investigation was to attempt to provide reasonable explanations for the anodic peaks at ≈ 400, 460 and 560 mV on the second and later cycles.

Figure 2 shows similar voltammograms recorded for a slightly more aged sample of β-$Ni(OH)_2$ (type B). The overall pattern of behaviour is similar to that found in Fig. 1. In the case of sample B, the oxidation processes on the first cycle are not resolved but can be shown as previously [1] to reach maxima at 590 and 660 mV, respectively. As a consequence of the increased difficulty in converting V_β to V_γ the cathodic peaks in Fig. 2 are much broader owing to the reduction of a mixture of phase V_β and V_γ. The system is also

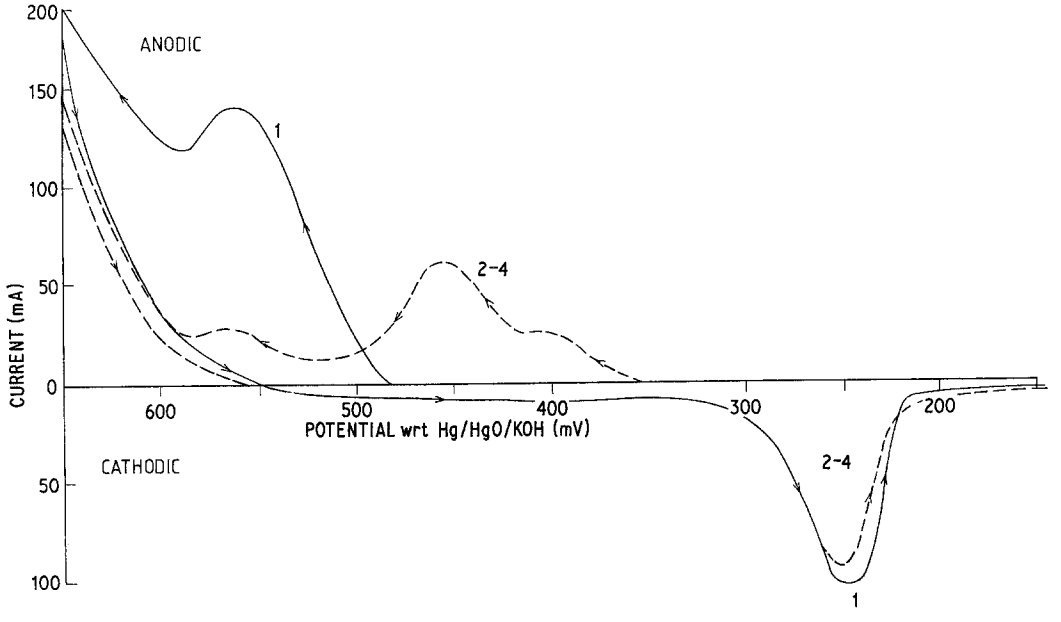

Fig. 1. Cyclic voltammogram for β-$Ni(OH)_2$, sample A, in 7 mol dm^{-3} KOH. Sweep rate 10 mV min^{-1}.

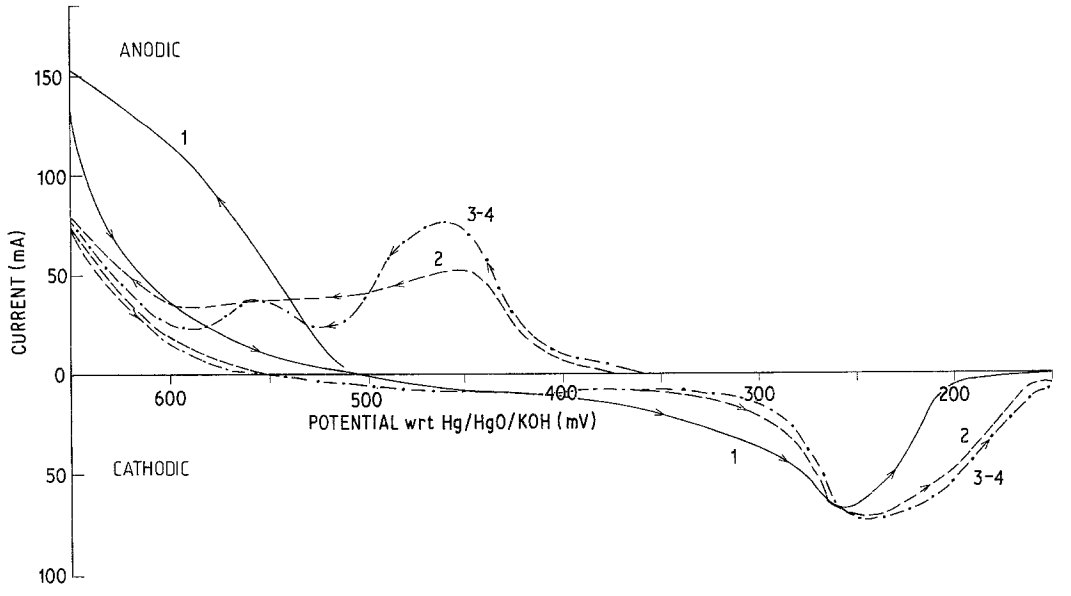

Fig. 2. Cyclic voltammogram for β-$Ni(OH)_2$, sample B, in 7 mol dm^{-3} KOH. Sweep rate 10 mV min^{-1}.

slower to reach stable voltammetric peak positions. However, by the third cycle anodic peaks can be observed in the same region as found for sample A with the exception that the peak at 400 mV is noticeably smaller appearing only as a shoulder in Fig. 2. As will be discussed presently the oxidation process at 400 mV is most likely to be due to oxidation of an α-phase material, U_α directly to the γ-phase, V_γ. Several investigators have demonstrated that electrochemically precipitated α-$Ni(OH)_2$ will undergo oxidation at this potential [5, 8–12]. The larger peak at 400 mV in Fig. 1 compared with Fig. 2 suggests that a greater quantity of the α-phase can be regenerated via the type A starting material compared to type B.

Similar results for sintered plate electrodes have been presented previously by MacArthur [13]. This author suggested reasonably that the anodic peak at $\approx$ 460 mV was due to oxidation of β-$Ni(OH)_2$ to β-NiOOH whilst the peak at $\approx$ 590 mV corresponded to further oxidation of β-NiOOH to the γ-phase. The main cathodic reduction peak at $\approx$ 250 mV was ascribed to reduction of the γ-phase.

3.2. *Coulometric measurements*

3.2.1. Electrodes pre-charged to give the γ-phase and then discharged. In order to make reliable assignments concerning the oxidation processes it is necessary to measure the charge relating to each peak. Figure 3 shows an *I–E* curve obtained using combined linear sweep voltammetry and oxygen volume measurements at a sweep rate of

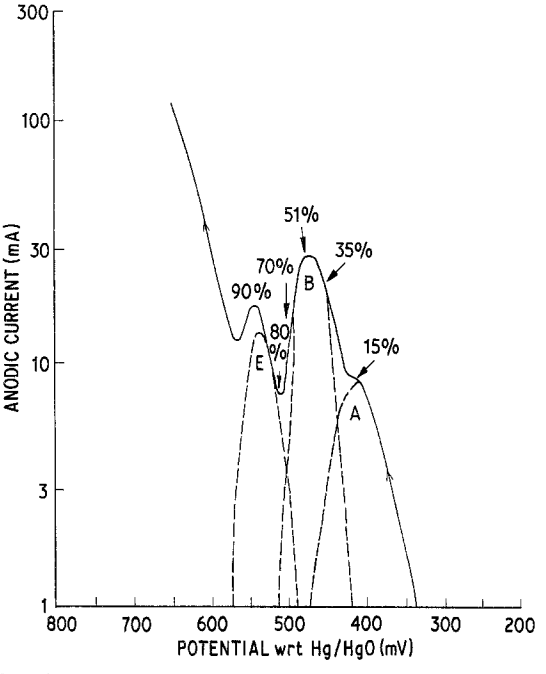

Fig. 3. Positive going linear sweep for pre-treated electrode, sample B, taken to various charge inputs (%) indicated on diagram. Electrodes pre-charged to give the γ-phase and discharged before use. Sweep rate 2 mV min^{-1}. – – – – –, deconvoluted peaks after removal of oxygen current component.

2 mV min^{-1} for a sample of the pre-treated electrode material (from type B) immediately after the conditioning discharge. In common with several voltammograms to be presented, the current is plotted on a logarithmic scale. The broken lines indicate likely peak deconvolutions after removal of the oxygen evolution current component [1]. Percentage figures indicated at various stages along the curve represent the quantity of charge accepted on recharging given by:

$$\frac{\text{(charge accepted on anodic cycle)}}{\text{(charge removed on cathodic cycle after the electrode had been pre-charged to an oxidation state of 3.54)}} \times 100\%$$

Three anodic peaks A, B and E can be clearly identified at ≈ 420, 470 and 550 mV before oxygen evolution predominates. The quantities of charge relating to peaks A, B and E amount to 19, 39 and 21 coulombs (C) respectively. A one electron change for this electrode sample would require 84.6 C.

If the peak B at 470 mV was due to oxidation of β-$Ni(OH)_2 \rightarrow \beta$-NiOOH involving a 1e change and peak E at 550 mV was due to further oxidation of β-NiOOH to a γ-phase of oxidation state 3.54 (i.e., a 0.54 e change) then a peak E:peak B ratio of 0.54 would be expected. The experimentally measured ratio of 0.538 is in apparent agreement with this simplified hypothesis.

Figure 4 shows an anodic voltammogram obtained at a slightly faster sweep rate of 10 mV min^{-1} for the same type of electrode sample used to generate Fig. 3. The peaks B and E can be clearly identified at 490 and 570 mV but peak A at 400 mV although present is less clearly resolved. In general, slow sweep rates are desirable to obtain the maximum resolution of peaks by minimising double layer charging and potential distribution through the porous electrode structure. This requirement must, however, be balanced against the time taken to perform the sweep and the transformation of unstable phases. The peaks E and B involve ≈ 18 and 44 C respectively giving a peak E:peak B charge ratio of 0.41.

By allowing the electrode to stand in the discharged state for 4 h rather than using immediately after the conditioning charge/discharge cycles an additional peak could be resolved in the oxidation

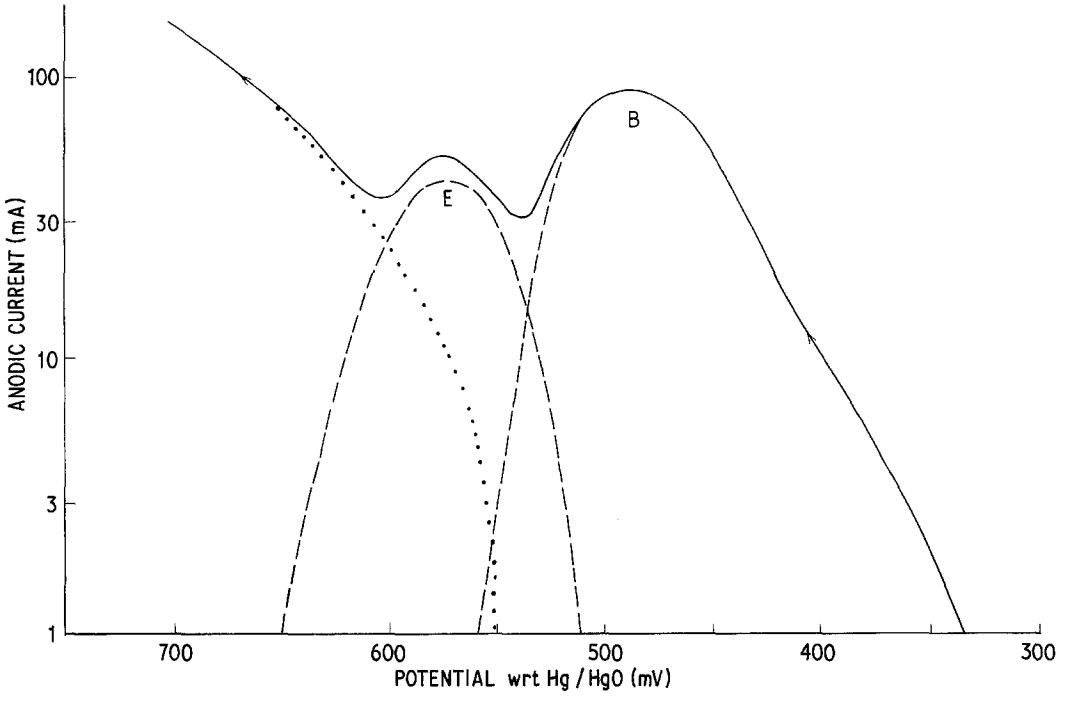

Fig. 4. Positive going linear sweep for pre-treated electrode sample B. ....., oxygen current component; – – – –, deconvoluted peaks after removal of oxygen current component. Electrodes pre-charged to give the γ-phase and discharged before use. Sweep rate 10 mV min^{-1}.

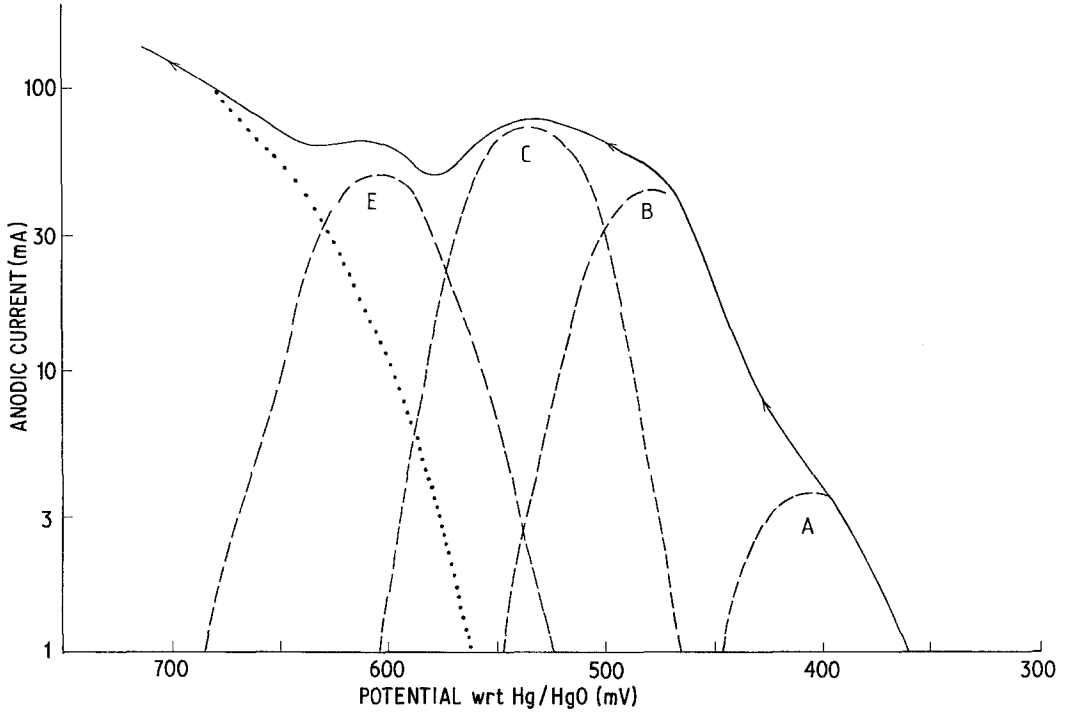

Fig. 5. As for Fig. 4, but with the electrode allowed to stand in a discharged state for 4 h before the anodic sweep.

envelope even at 10 mV min^{-1} as shown in Fig. 5. Four anodic processes A, B, C and E can now be observed at 400, 490, 530 and 600 mV. Corresponding charge quantities relating to these deconvoluted peaks amount to 1, 19, 29 and 22 C, respectively. The oxidation process at 400 mV as expected now involves only a small proportion of the overall charge. This observation demonstrates clearly the instability of the α-phase, U_α. The transformation of electrochemically precipitated α-phase materials has been shown previously [5] to be a fairly rapid first order process, a typical half-life being ≈ 20 min in 7 mol dm^{-3} KOH at room temperature.

The results of Fig. 5 suggest that more than one oxidation process can take place in the region of 500 mV. The peak area ratios E:B or E:C exceed the value of 0.54, but the combined ratio E:(B + C) amounts to 0.46.

3.2.2. Cathodic behaviour. In an attempt to identify the species present at various stages of oxidation several electrodes were charged to the points indicated previously in Fig. 3 and then swept cathodically. The resulting cathodic voltammograms at 2 mV min^{-1} are shown in Figs. 6–8.

The electrode having a 15% charge input corresponding to the peak A maximum at ≈ 400 mV in Fig. 3 gave a cathodic peak at 310 mV as shown in Fig. 6a. On increasing the charge input to 22% and then 35% (ascending peak B of Fig. 3) there is a marked displacement of the reduction process to less cathodic potentials (Figs. 6b and c). Fig. 6c shows two distinct reduction processes at 350 and ~ 400 mV respectively. It has been demonstrated previously [1] that coexisting phases within the β-phase system can undergo reduction at potentials between 400 mV and 350 mV depending on the free energy change for the process $V_\beta \rightleftharpoons U_\beta$. It has also been shown that the γ-phase, V_γ also undergoes reduction at potentials of ~ 300 mV and below.

Thus the reduction process at 310 mV in Fig. 6a relating to peak A of Fig. 3 can reasonably be ascribed to reduction of the γ-phase ($V_\gamma^A \rightarrow U_\alpha^A$). Figures 7d, e and f show the cathodic voltammograms for charge inputs of 51, 70 and 80% respectively. These values correspond to the peak B maximum at ≈ 490 mV and the region before peak

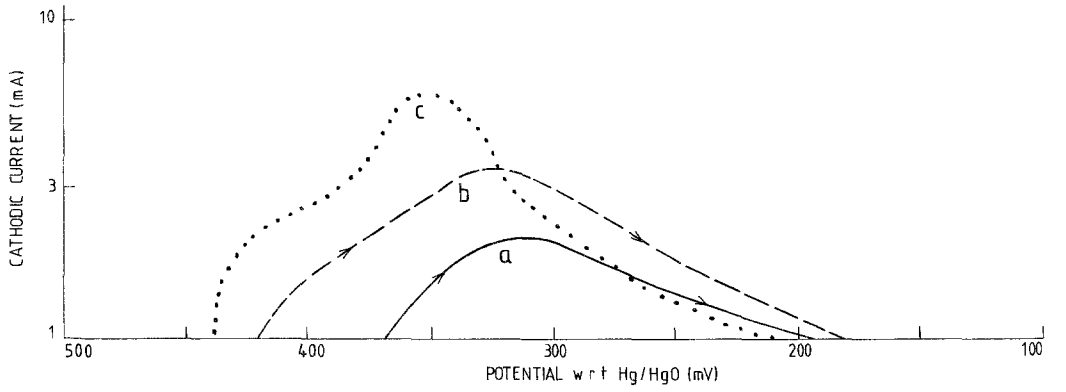

Fig. 6. Cathodic linear sweeps for electrodes taken to various fixed charge points indicated in Fig. 3. Sweep rate 2 mV min^{-1}. (a) ———, 15% charge input; (b) – – – –, 22% charge input; (c) ....., 35% charge input.

E of Fig. 3. The cathodic curves reveal that the reduction process relating to the latter part of peak B now shifts progressively in the opposite direction to more cathodic potentials resting at 310 mV. This is the same potential as that observed for the discharge process relating to anodic peak A at 400 mV. Clearly anodic peak B at 470 mV must be composed of two overlapping processes. The initial part of peak B relates to oxidation of U_β^B to V_β^B within the β-phase system whilst the latter part (resolved in favourable cases as peak C) relates to formation of a γ-phase V_γ^C most probably by direct oxidation of phase U_α^C. It is likely that phase U_α^C is of the so called 'deactivated' type [2, 5, 6] derived initially from the unstable phase U_α^A. It is not clear as yet whether the oxidised phases V_γ^C and V_γ^A have any significant structural difference.

Figures 8g and h show cathodic voltammograms after 90 and 100% charge inputs relating to peak E of Fig. 3. In spite of the relatively small additional charge accepted a sudden shift in the main cathodic reduction process from 310 to 250 mV is observed. There is also evidence of a residual reduction process in the region of 400–310 mV. The less positive position of the main reduction peak is as would be expected for the reduction of a γ-phase which is consistent with the known final oxidation state relating to peak E

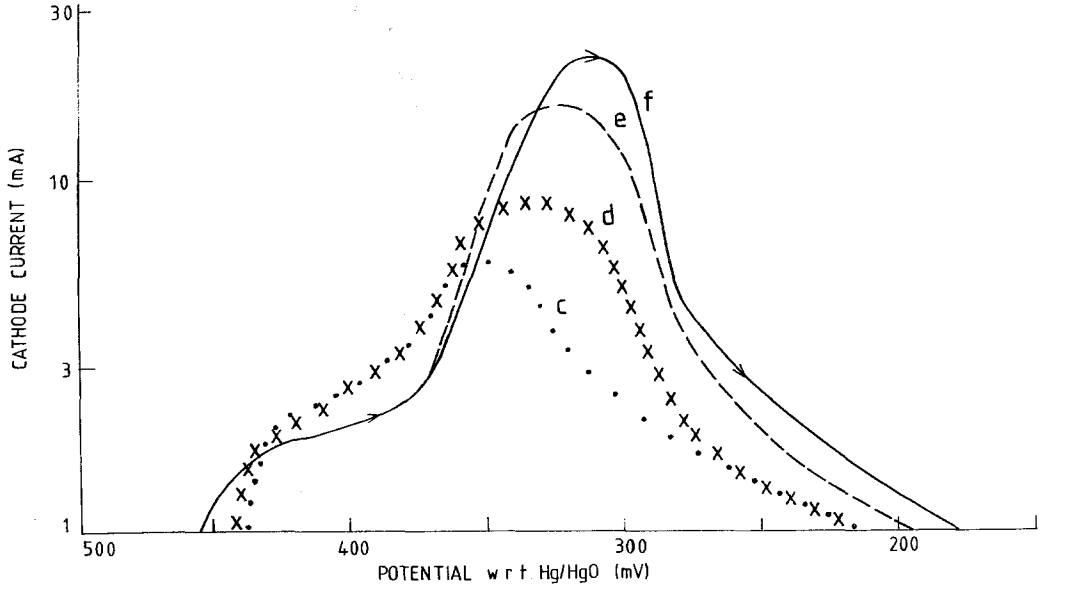

Fig. 7. As for Fig. 6. (c) ....., 35% charge input; (d) x x x x, 51% charge input; (e) – – – –, 70% charge input; (f) ———, 80% charge input.

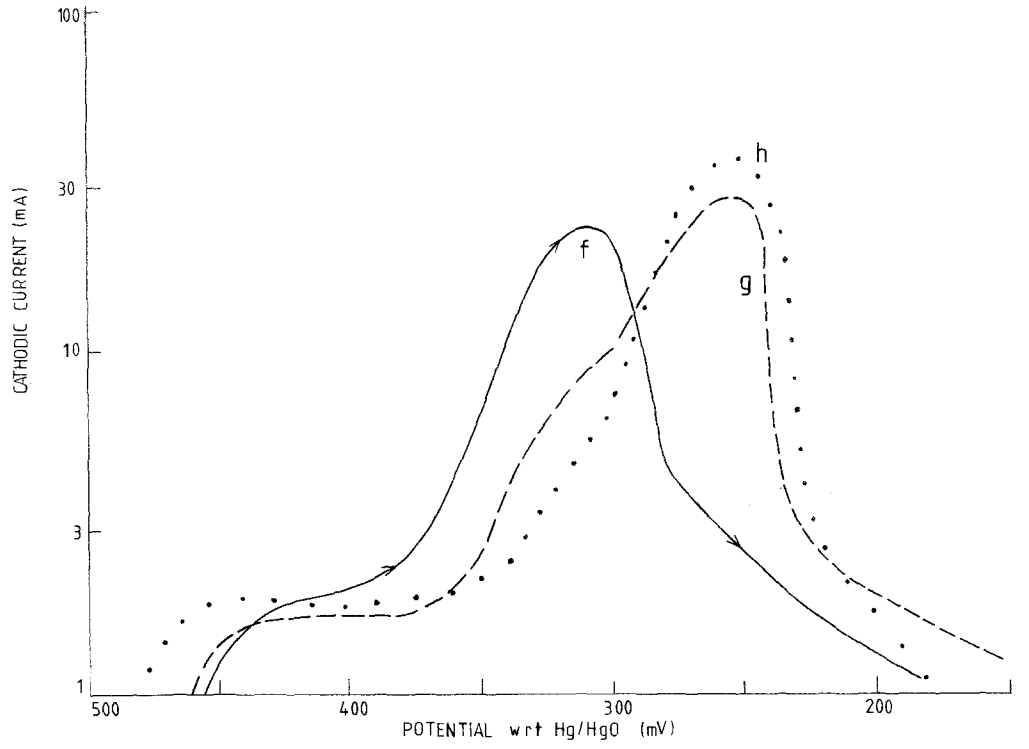

Fig. 8. As for Fig. 6. (f) ———, 80% charge input; (g) – – – –, 90% charge input; (h) ....., 100% charge input.

of Fig. 3. Clearly γ-phases can undergo reduction over a range of potentials between 300 and 200 mV. This observation suggests that the γ-phase V_γ^E produced at high anodic potential via the intermediate β-phase V_β^B, i.e., $V_\beta^B \rightarrow V_\gamma^E$ has a different free energy of formation compared with that formed at less positive potentials by direct oxidation of U_α^A or U_α^C. Furthermore, the magnitude of the reduction peak at 250 mV in Figs. 8g and h suggest that after oxidation at high anodic potentials the phases V_α^A or V_γ^C also undergo a structural modification such that the final product is largely V_γ^E.

From the above discussion it is apparent that the overall oxidation process is considerably more complicated than previously supposed particularly with respect to the possible reactions occurring in the region of 500 mV. Accordingly we propose an alternative scheme summarized in Tables 1 and 2 relating to Figs. 3 and 5 respectively. In Table 1 peak B is unresolved and includes both the oxidation processes $U_\beta^B \rightarrow V_\beta^B$ and $U_\alpha^C \rightarrow V_\gamma^C$. In Table 2 the process $U_\alpha^C \rightarrow V_\gamma^C$ is resolved and assigned separately to peak C.

The least oxidised co-existing phases of the types U_β^B and U_α^A (or U_α^C) have been shown [4] to have an oxidation state of 2.25. Phases V_γ^E, V_γ^C or V_γ^A have been shown to have oxidation states of at least 3.54. The oxidation state of phase V_β^B is uncertain but is likely to be between 2.75 and 3.0.

Table 1. Anodic peak assignments for electrodes pre-charged to the γ-phase and then discharged before use (see also Fig. 3). The co-existing phases are assumed to have compositions of the general types; V_β^B, V_β^D = $[0.9NiOOH{\cdot}0.1Ni(OH)_2]0.21H_2O{\cdot}0.03KOH$; U_β^B, U_β^D = $[0.25NiOOH{\cdot}0.75Ni(OH)_2]0.25H_2O$; V_γ^A, V_γ^C, V_γ^E = $[0.833NiO_2{\cdot}0.166Ni(OH)_2]0.35H_2O{\cdot}0.33KOH$; U_α^A, U_α^C = $[0.125NiO_2{\cdot}0.875Ni(OH)_2]0.67H_2O$. *The co-existing phases* U_β^B, U_β^B, U_α^A *and* U_α^C *have nickel oxidation states of 2.25 [4]. Phases* V_γ^A, V_γ^C, V_γ^E *have oxidation states of at least 3.54 whilst phases* V_β^B *and* V_β^D *are likely to have oxidation states between 2.75 and 3.0.*

Peak	*Potential* (mV)	*Charge* (C)	*Process*
A	400	19	$U_\alpha^A \rightarrow V_\gamma^A$
B	470	39	$U_\beta^B \rightarrow V_\beta^B$ $U_\alpha^C \rightarrow V_\gamma^C$
E	550	21	$V_\beta^B \rightarrow V_\gamma^E$

Table 2. Anodic peak assignments for electrodes pre-charged to the γ-phase, discharged and allowed to stand for 4 hours before use (see also Fig. 5)

Peak	*Potential* (mV)	*Charge* (C)	*Process*
A	400	1	$U_{\alpha}^{A} \rightarrow V_{\gamma}^{A}$
B	490	19	$U_{\beta}^{B} \rightarrow V_{\beta}^{B}$
C	530	29	$U_{\alpha}^{C} \rightarrow V_{\gamma}^{C}$
E	600	22	$V_{\beta}^{B} \rightarrow V_{\gamma}^{E}$

If the oxidation state of V_{β}^{B} is assumed to be 2.9 then the oxidation process $U_{\beta}^{B} \rightarrow V_{\beta}^{B}$ involves a ≈ 0.65 e change whilst the process $V_{\beta}^{B} \rightarrow V_{\beta}^{E}$ involves a 0.64 e change. Accordingly a peak E: peak B ratio nearer unity would be expected where the process $U_{\beta}^{B} \rightarrow V_{\beta}^{B}$ is separately resolved.

Examination of Table 2 indicates that the peak E:peak B ratio is 1.16 in reasonable accord with likely co-existing phase compositions. Recent studies [14] have independently confirmed that certain varieties of β-$Ni(OH)_2$ and α-$Ni(OH)_2$ can oxidise at ≈ 470 mV but to give different products. Furthermore, so called 'activated' and 'deactivated' α-$Ni(OH)_2$ can both be shown to oxidise directly to a γ-phase having an oxidation state of at least 3.5. These observations add credance to the likelihood of overlap in oxidation reactions between the U_{β}/V_{β} and U_{α}/V_{γ}-phase systems in the region near 470 mV.

The fact that the peakE:peak B or peak E: (peak B + peak C) charge ratios for cycled electrodes close to 0.54 may be observed in some cases, as in the case of electrodes on the first cycle starting with β-$Ni(OH)_2$ [1], must be regarded as fortuitous. The simplified model assumes that the oxidized phases revert completely to a single variety of β-$Ni(OH)_2$ after discharge. In practice high residual oxidation states are encountered (≈ 2.6) due to the presence of a large amount of unreduced γ-phase and a mixture of the least oxidized coexisting phases U_{α} and U_{β} belonging to both the α- and β-structural types.

3.2.3. Electrodes pre-cycled within the β-phase system. Fig. 9 shows an oxidation curve obtained

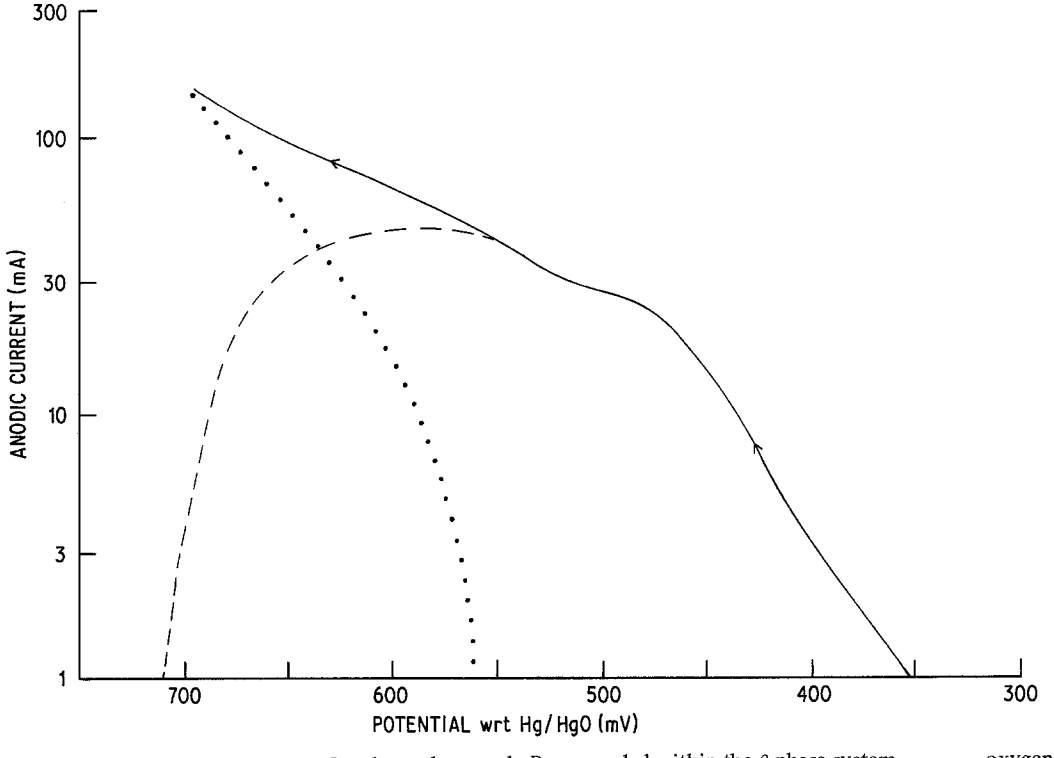

Fig. 9. Positive going voltammogram for electrode, sample B, pre-cycled within the β-phase system. ....., oxygen current component – – – –, active material oxidation envelope. Sweep rate 10 mV min^{-1}.

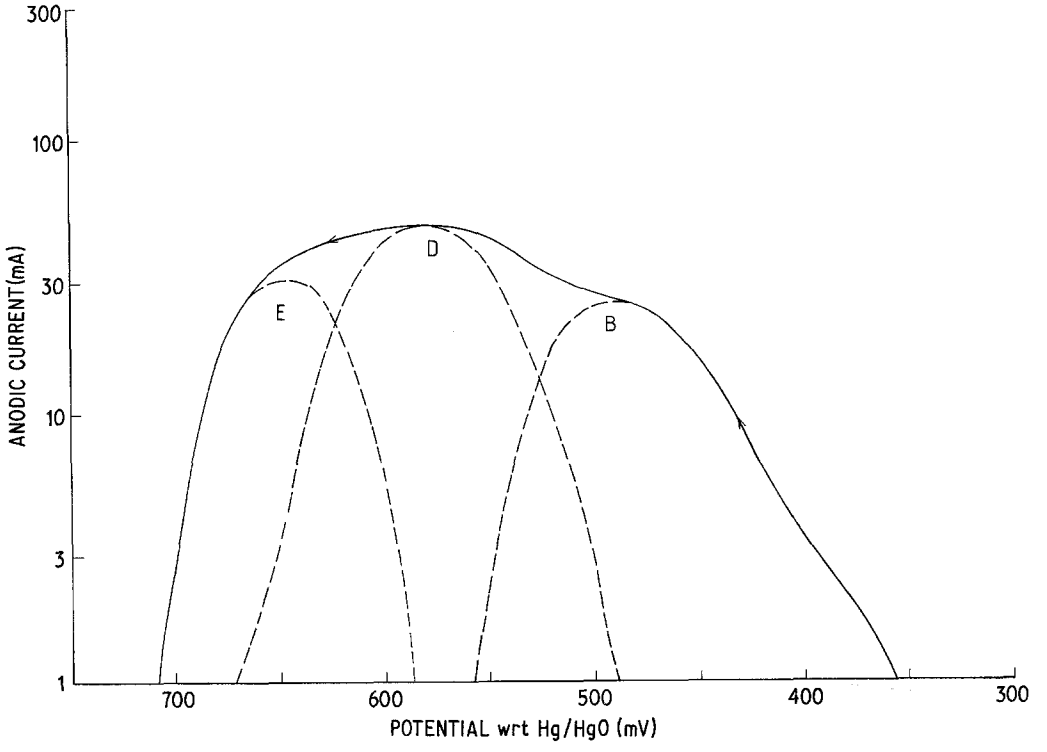

Fig. 10. As for Fig. 9. showing deconvoluted peaks (– – –).

using combined linear sweep voltammetry ($10\,mV\,min^{-1}$) and oxygen evolution measurements for a sample of the above pre-cycled electrode material. The behaviour of electrodes of this type resembles that described previously [1] using β-$Ni(OH)_2$ as a starting material. Distinct anodic peaks are not observed directly without removal of the contribution due to oxygen evolution as indicated by the broken line. The nickel oxidation state present in the electrode at the end of the positive going sweep was 3.54 indicating that the final product was the γ-phase, V_γ^E. After removal of the oxygen evolution current component, the active material oxidation envelope can be obtained as in Fig. 10. This envelope can be regarded as being composed of three overlapping peaks B, D and E (with peak A as a minor contributor) at 490, 580 and 650 mV respectively. The broken lines in Fig. 10 show our proposed deconvolutions assuming symmetrical peaks. The positions of peaks D and E are drawn to be close to those found when using β-$Ni(OH)_2$ as a starting material [1]. The peak B including the very small shoulder A at ~ 400 mV is clearly due to an additional process.

In order to make likely peak assignments it is necessary to calculate the areas under peaks B, D and E and compare these with those expected theoretically.

By analogy with the behaviour of pure β-$Ni(OH)_2$ on the first anodic cycle the peaks D and E could be reasonably related in the first instance to the processes $U_\beta^D \rightarrow V_\beta^D$ and $V_\beta^D \rightarrow V_\gamma^E$ respectively. The process $U_\beta^D \rightarrow V_\beta^D$ is considered to have a different free energy of reaction compared to the process $U_\beta^B \rightarrow V_\beta^B$ observed at lower anodic potentials and already discussed. Phase U_β^B can be regarded as being a more 'activated' type compared to U_β^D.

An electrode initially having an oxidation state of 2.65 (e.g., the starting material) would have been expected to contain $\approx 62\%$ of phase V_β^B and 38% U_β^D assuming uncharged β-$Ni(OH)_2$ to be absent. This latter assumption appears to be reasonable provided the average oxidation state of the electrode is taken initially above 2.6. As a result of cyclic charge/discharge, the phase V_α^B is considered to give rise progressively to the more 'activated', phase U_β^B as discussed previously [1]. If it is furthermore assumed that phase U_β^B is only

Table 3. Possible anodic peak assignments for electrodes pre-cycled within the β-phase system (see also Fig. 10)

Scheme Number	Process	Potential (mV)	Peak areas (C) Calculated		Experimental
1	$U_\beta^B \rightarrow V_\gamma^B$	490	75		28
	$U_\beta^D \rightarrow V_\beta^D$	580	21		54
	$V_\beta^D \rightarrow V_\gamma^E$	650	25		25
2	$U_\beta^B \rightarrow V_\beta^B$	490	34		28
	$U_\beta^D \rightarrow V_\beta^D$	580	19		54
	$V_\beta^D \rightarrow V_\gamma^E$	650	65		25
3	$U_\beta^B \rightarrow V_\beta^B$	490	34		28
	$U_\beta^D \rightarrow V_\beta^D$	580	24	61	54
	$V_\beta^B \rightarrow V_\gamma^D$		37		
	$V_\beta^D \rightarrow V_\gamma^E$	650	25		25

produced via discharge of phase V_β^B (i.e. it is distinguishable from U_β^D formed on the first cycle) then the starting material having an average oxidation state of 2.32 would contain 11% phase V_β^B, 51% phase U_β^B and 38% phase U_β^D. Depending on whether phase U_β^B oxidizes directly to a γ-phase or indirectly via a β-phase, three hypothetical routes can be proposed as summarized in Table 3.

It is clear from the results presented in Table 3 that route 1, where the 'activated' phase U_β^B charges directly to the hypothetical phase V_γ^B cannot be responsible for peak B. In both routes 2 and 3 phase U_β^B is assumed to oxidize to phase V_β^B before further oxidation to phase V_γ^D or V_γ^E. Route 3 shows the most satisfactory agreement between the calculated and experimentally observed peak areas. This mechanism proposes an overlapping pair of consecutive oxidation reactions in which γ-phase formation can take place at least at two different potentials. The scheme is further complicated by the ability of one of these conversions to take place at a similar potential to the process $U_\beta^D \rightarrow V_\beta^D$ observed predominantly on the first cycle at ≈ 580 mV. These results clearly require the coexisting phase pairs to have different free energies of formation.

In the previous section 3.2.2 it was suggested that the γ-phase, V_γ^E formed at high positive potential probably differs significantly in free energy from those produced at lower anodic potentials (V_γ^A, V_γ^C or V_γ^D). These γ-phases may differ slightly in oxidation state or water and alkali content. Bode *et al.* [9, 10] have identified two structurally different types described as γ_1 and γ_2. It is also possible that the phases V_β^D and V_β^B have slightly different structures although direct chemical evidence so far is lacking.

Arvia *et al.* [15–18] have similarly observed multiple anodic and cathodic peaks during cyclic voltammetry using thin film $Ni(OH)_2$ electrodes. Three cathodic peaks were considered to arise from reduction of nickel oxyhydroxide species having the same overall oxidation state (Ni^{3+}) but different energetic configurations [15]. The degree of hydration of the $Ni(OH)_2$ species was considered to influence the course of the oxidation process. The overall concept proposed by Arvia *et al.* [15–18] is superficially similar to that proposed in this and our previous studies [1–6] in which coexisting phases having a range of free energies of formation can be developed from α or β-$Ni(OH)_2$ parent layer lattices.

Regrettably, in the work of Arvia *et al.* [15–18] neither the precise oxidation state or identity of the phases was established by independent means. In 0.1 mol dm^{-3} KOH with K_2SO_4 supporting electrolyte Arvia *et al.* [15] observed cathodic peaks at 630, 585 and 510 mV with respect to NHE (or 532, 487 and 412 mV with respect to Hg/HgO/KOH). The largest peak was found for the thin film electrodes at 630 mV NHE giving a reversal in the peak height order generally observed for the bulk materials. Arvia *et al.* suggested that the peaks at 630 and 585 mV NHE are likely to be due to reduction of γ-phases having different crystal structures (i.e. the γ_1 and γ_2 varieties described by Bode *et al.* [9, 10]). The peak at the most cathodic potential (510 mV) was assigned to the reduction of β-NiOOH.

The peak assignments given in this and our previous study [1] are consistent with the reversible potentials measured for various U_α/V_γ and U_β/V_β couples using sintered plate electrodes in a variety of alkali types [2–6]. If the assignments of Arvia *et al.* are justified then it must be concluded that thin nickel hydroxide layers on nickel behave kinetically and thermodynamically in a different way to the bulk phases.

4. Conclusions

Depending on the positive limit and charge applied to the β-$Ni(OH)_2$ starting material, several anodic and cathodic peaks can be observed. When the reduced phases present in the pre-cycled electrode belong to the β-type anodic processes at $\approx$490, 580 and 650 mV wrt Hg/HgO/7 mol dm^{-3} KOH can be identified. The process at 490 mV can be ascribed to oxidation of an 'activated' phase U_β^B to phase V_β^B involving only Ni^{2+} and Ni^{3+} species. At 580 mV a similar process takes place namely $U_\beta^D \rightarrow V_\beta^D$ involving species having a different free energy of formation but this process overlaps another involving further oxidation of β-phase, V_β^B to a γ-phase V_γ^D, containing Ni^{4+} species. The most anodic process at 650 mV then involves further oxidation of phase V_β^D to V_γ^E.

A similar but more complex sequence of overlapping oxidation processes are also found when the starting material contains a mixture of both α- and β-reduced phases. The α-phase materials are derived on discharge of the γ-phases produced on previous cycles at high anodic potentials. Four anodic peaks at $\approx$400, 490, 530 and 600 mV can be found relating to the following processes at increasingly positive potential, $U_\alpha^A \rightarrow V_\gamma^A$, $U_\beta^B \rightarrow V_\beta^B$, $U_\alpha^C \rightarrow V_\gamma^C$ and $V_\beta^B \rightarrow V_\gamma^E$. The processes $U_\alpha^A \rightarrow V_\gamma^A$ and $U_\alpha^C \rightarrow V_\gamma^C$ involve direct oxidation of Ni^{2+} to Ni^{4+} species. Species U_α^A and U_α^C can be regarded as 'activated' and 'deactivated' types respectively. There is evidence to suggest that the phases V_α^A or V_γ^C have a different free energy of formation compared with V_γ^E. Phases V_γ^A and V_γ^C appear to transform to V_γ^E at high anodic potentials. These different forms may perhaps be identified with the structural classes designated γ_1 and γ_2 by Bode *et al.* [9, 10]. It is also evident that the pairs of coexisting phases within the β-phase system namely U_β^B/V_β^B and U_β^D/V_β^D have different free energies of reaction as discussed previously [1].

Whilst the oxidised β-phases V_β^B or V_β^D can be intermediates during the formation of the γ-phases these materials contrary to common belief are not essential intermediates on the reverse cycle. Reduction of the γ-phase can occur via direct reduction of Ni^{4+} to Ni^{2+} species. The involvement of 2 electrons in the reaction determining the reversible potential for the U_α/V_γ couples has been confirmed previously [4].

When the oxidation state of the active material exceeds 3.54 and the final product is the γ-phase V_γ^E only a single reduction peak is found at $\approx$0.25 V ($V_\gamma^E \rightarrow U_\alpha^A$). The phase U_α^A is unstable and may revert chemically to U_α^C or U_β^B.

By interrupting the anodic scan after various states of charge have been reached it is possible to identify the anodic products by subsequent reverse scans. Those belonging to the β-class usually give peaks at less cathodic potentials whilst the γ-class give reduction peaks at the most cathodic potentials. The relative movement of the cathodic peaks observed is consistent with the anodic peak assignments proposed. The cathodic peaks at $\approx$400, 320, 300 and 250 mV can be assigned to the processes $V_\beta^D \rightarrow U_\beta^D$, $V_\beta^B \rightarrow U_\beta^B$, $V_\gamma^A \rightarrow U_\alpha^A$ or $V_\gamma^C \rightarrow U_\alpha^C$ and $V_\gamma^E \rightarrow U_\alpha^A$ respectively.

Acknowledgements

The authors wish to thank the Directors of Berec Group Limited for permission to publish this work and Dr. F. L. Tye for helpful discussions. We also thank Mr. M. J. O'Donoghue for experimental contributions.

References

[1] R. Barnard and C. F. Randell, paper presented at Electrochemical Energy Storage 1981, *J. Power Sources*, in press.
[2] R. Barnard, C. F. Randell and F. L. Tye, *J. Appl. Electrochem.* **10** (1980) 109.
[3] *Idem, ibid.* **10** (1980) 127.
[4] *Idem, J. Electroanal. Chem.* **119** (1981) 17.
[5] *Idem*, in 'Power Sources 8', (edited by J.Thompson) Academic Press, New York (1981) p. 401.
[6] *Idem, J. Appl. Electrochem.* **11** (1981) 517.
[7] R. Barnard, G. T. Crickmore, J. A. Lee and F. L. Tyle, *J. Appl. Electrochem.* **10** (1980) 61.
[8] D. M. MacArthur, *J. Electrochem. Soc.* **117** (1970) 422.
[9] H. Bode, K. Dehmelt and J. Witte, *Electrochim. Acta* **11** (1966) 1079.
[10] *Idem, Z. Anorg. Chem.* **366** (1969) 1.
[11] G. W. D. Briggs, 'Electrochemistry', Vol. 4. Specialist Periodical Reports, The Chemical Society, London (1974), p. 33.
[12] D. F. Pickett and J. T. Malloy, *J. Electrochem. Soc.* **125** (1978) 1026.
[13] D. M. MacArthur, in 'Power Sources 3' (edited by D. H. Collins) Oriel Press, Newcastle (1971) p. 91.
[14] R. Barnard, C. F. Randell and F. L. Tye, paper pre-

sented at the Denver Colorado Meeting of the Electrochemical Society (1981).
[15] R. S. Schrebler-Guzman, J. R. Vilche and A. J. Arvia, *J. Electrochem. Soc.* **125** (1978) 1578.
[16] *Idem, Corros. Sci.* **18** (1978) 778.
[17] *Idem, J. Appl. Electrochem.* **9** (1979) 183.
[18] *Idem, ibid.* **9** (1979) 321.